Heliyon 5 (2019) e02091

Contents lists available at ScienceDirect

Heliyon

journal homepage: www.heliyon.com

Effect of yttrium ion on the properties of tri ethyl ammonium picrate single crystals

S. Velayutham, M. Selvapandiyan *

Department of Physics, Periyar University PG Extension Centre, Dharmapuri, 636-701, Tamil Nadu, India

ARTICLE INFO

Keywords:
Materials Science
Slow evaporation
Powder XRD
UV –visible
PL
FTIR
EDAX
Materials Application
Materials Characterization
Materials Property
Materials Structure
Materials Synthesis

ABSTRACT

Tri Ethyl Ammonium Picrate (TEAP) and Yttrium (Y^{2+}) ions doped single crystals were grown by slow evaporation technique at room temperature. The estimated band gap of the pure TEAP, 0.10 mol % and 0.15 mol % of Y^{2+} ions doped TEAP are 3.76 eV, 3.82 eV and 3.86 eV. Crystallite size of the grown materials was calculated from powder XRD as 1.456 nm for TEAP, 3.2028 nm for 0.10 mol % of Y^{2+} ions doped TEAP and 6.934 nm for 0.15 mol % of Y^{2+} ions doped TEAP single crystals. Y–O stretching mode was assigned by FTIR spectral peak at 549 cm^{-1}. The PL excitation wavelength of the grown materials is 350 nm. The EDAX analysis confirmed by the Carbon, Nitrogen, Oxygen and Yttrium were presented in grown crystals.

1. Introduction

Nonlinear optical materials have been synthesized and grown by many researchers for the past four decades due to their versatile properties such as low laser damage threshold, high third order nonlinear optical susceptibility, and high chemical flexibility [1, 2]. Due to unique properties, the multifunctional NLO material attracts the number of fields of applications like Optical signal processing, Optical switching, Lasers, Sensors, Environment monitors and Optical communications, Optical memory, Optical modulating, Optical storage technology and Optical limiting [3, 4, 5, 6, 7, 8, 9, 10]. Organic nonlinear optical materials are high quality in nature due to π-electron delocalization which means that the valance free electron is interacting with neighbouring electron and enhances the properties of the materials [11]. The phenolic group might favour the formation of hydrogen-bonding interactions to increase the molecular hyperpolarizability and NLO effects [12]. Nonlinear optical response of Tri Ethyl Ammonium Picrate single crystal is 1.5 times as larger than that of KDP [13]. A number of works such as 3-Methyl anilium picrate [14], 1, 3 –Dimethyl urea dimethyl ammonium picrate [15] have been already reported. Based on the literature survey and the knowledge of the authors, no researcher has analysed Tri Ethyl Ammonium Picrate (TEAP) and Y^{2+} ions doped TEAP and characterised by PL, EDAX, FTIR, and UV –visible technique. In this present investigation, Tri Ethyl Ammonium Picrate, 0.10 mol % and 0.15 mol % of Y^{2+} ions doped single crystals were grown. The properties of grown crystal were analysed by Powder XRD, UV –visible, FT-IR, PL, and EDAX. The obtained results of grown materials were reported in this article.

2. Experimental

Single crystals of TEAP were grown by slow evaporation method [16] at room temperature from the calculated amount of AR of grade Tri Ethyl Amine and Picric Acid. Initially 6.97 ml of Tri Ethyl Amine and 22.9 g of picric acids was dissolved in equal mixture of deionised water (50 ml) and ethanol (50 ml) in the molar ratio of 1:1. The mixed solution was stirred continuously for 6 h at 60 °C for getting homogeneous saturated solution. The saturated solution was filtered with the help of Whattman Filter paper (125 mm dia) and kept unperturbed place for evaporation. At the end of 40^{th} day the transparent yellow coloured TEAP crystals with size of $8 \times 7 \times 5$ mm^3 was harvested. Again TEAP solution was prepared as per above procedure in two different beakers and then slowly added 0.10 and 0.15 mol % of Yttrium Oxide and stirred continuously about an

* Corresponding author.
E-mail address: mselvapandiyan@rediffmail.com (M. Selvapandiyan).

https://doi.org/10.1016/j.heliyon.2019.e02091
Received 30 November 2018; Received in revised form 3 April 2019; Accepted 12 July 2019

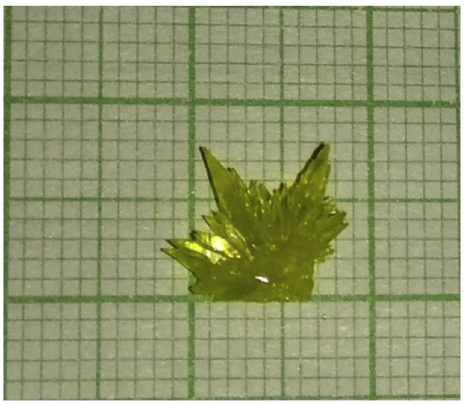

(a) As grown TEAP

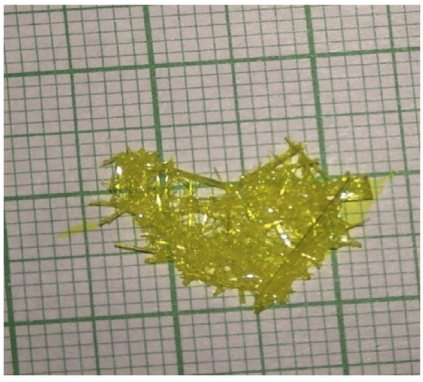

(b) As grown 0.10 mol % of Y^{2+} doped TEAP

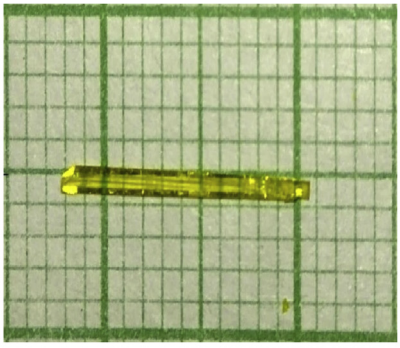

(c) As grown 0.15 mol % of Y^{2+} doped TEAP

Fig. 1. As grown: **(a)** TEAP (**b)** 0.10 mol % of Y^{2+} doped TEAP and **(c)** 0.15 mol % of Y^{2+} doped TEAP.

hour to get completely saturated homogeneous solution. Then clear solution was filtered and kept for evaporation in unperturbed place. The 0.10 and 0.15 mol % of Y^{2+} ions doped TEAP crystals were obtained at the end of 30^{th} day with the sizes about $5 \times 1 \times 1$ mm^3 and $13 \times 1 \times 1$ mm^3. The As grown TEAP, 0.10 mol % of Y^{2+} doped TEAP and 0.15 mol % of Y^{2+} doped TEAP were shown Fig. 1 (a, b & c). The grown crystals were subjected to various characterization studies such as Powder X-ray diffraction, FTIR, UV –visible, Photoluminescence and EDAX, and their detailed results are discussed in this article.

3. Results and discussion

3.1. Powder X-ray diffraction studies

Powder X-ray diffraction studies have been carried out to confirm the crystallinity of the grown crystals by using The X-Pert PRO family of multipurpose PAN analytical X-ray diffractometer with the wavelength of CuKα radiation ($\lambda = 1.54$ Å). The Powder XRD pattern of pure TEAP and Y^{2+} ions doped TEAP is shown Fig. 2. All the prominent peaks are

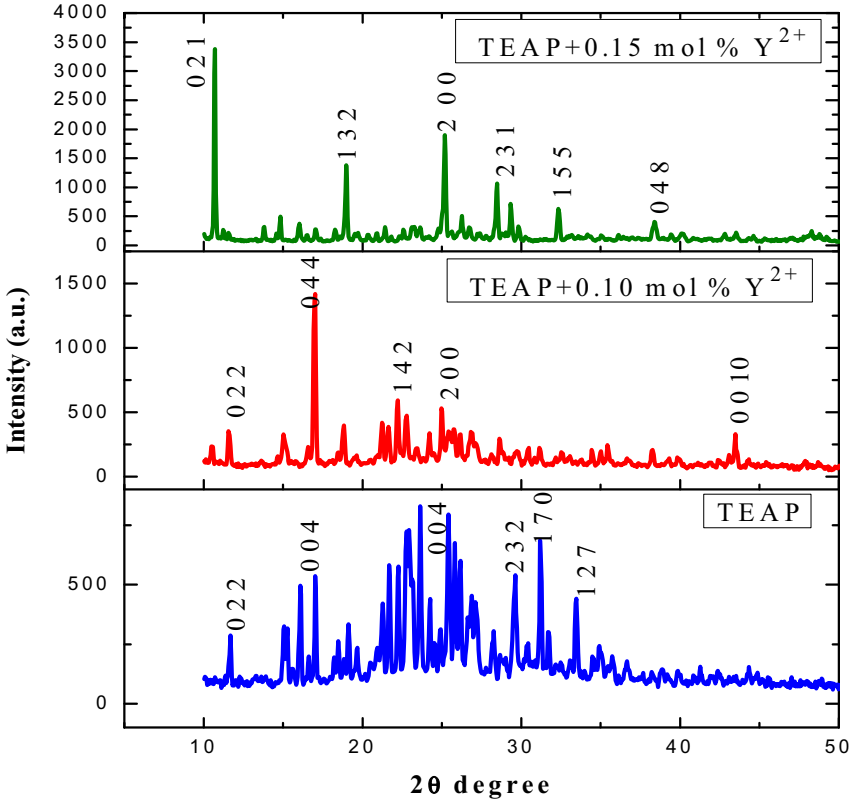

Fig. 2. Powder XRD Pattern of TEAP, 0.10 mol % Y^{2+} +TEAP and 0.15 mol % Y^{2+} +TEAP.

Table 1
An Average Crystallite size and lattice strain of the grown crystals.

S. No.	Crystals	2θ (degree)	Crystallite Size (nm)	Lattice Strain	Average Crystallite Size (nm)	Average Lattice Strain
1	Pure TEAP	17.02	1.44	0.1702	1.456	0.12522
		22.77	1.45	0.1300		
		23.63	1.45	0.1217		
		25.42	1.46	0.1129		
		31.17	1.48	0.0913		
2	0.10 mol % of Y^{2+}ions doped TEAP	11.57	3.13	0.1146	3.2038	0.06658
		17.02	3.15	0.0776		
		22.17	3.18	0.0593		
		25.02	3.19	0.0523		
		43.47	3.36	0.0291		
3	0.15 mol % of Y^{2+}ions doped TEAP	10.72	6.81	0.0570	6.934	0.03048
		18.97	6.87	0.0320		
		25.17	6.94	0.0239		
		28.47	6.99	0.0211		
		32.32	7.06	0.0184		

indexed with JCPDS card No 51–2120. Calculated lattice parameters of the grown crystals are a = 6.985 Å, b = 22.03 Å, c = 20.810 Å and α = β = γ = 90°. Lattice parameters confirm that the grown crystals belong to the system of Orthorhombic [17]. The doped crystals angles were slightly shifted and intensity of peaks varied due to concentrations of Y^{2+} ions in Tri Ethyl Ammonium Picrate, but not altered the crystal system of grown materials. High crystalline nature of the materials was confirmed by the well defined sharp peaks. The estimated average crystallite size and Lattice strain of the materials are 1.456 nm, 3.2038 nm, 6.934 nm and 0.12522, 0.06658, 0.03048 for pure TEAP, 0.10 mol % and 0.15 mol % of Y^{2+} ions doped TEAP single crystals. The estimated average crystallite size is high for 0.15 mol % of Y^{2+} ions concentrated materials which shows that the materials have higher quality structural nature than that of pure TEAP. **Under the assumption and Debye Sheerer formula, the crystallite sizes of the grown materials were calculated. An estimated Average Crystallite size and lattice strain of the grown crystals have presented in the** Table 1.

3.2. FTIR studies

Fourier transform infrared spectral studies of the grown Tri Ethyl Ammonium Picrate, 0.10 mol % and 0.15 mol % of Y^{2+} ions doped Tri Ethyl Ammonium Picrate single crystals was analysed by using Perkin Elmer spectrometer (version 10.4.00) in the range of 4000 cm^{-1} – 400 cm^{-1}. The analysed and recorded spectra of the grown crystals are depicted in Fig. 3. The peaks are found at 3433, 3091, 1632, 1559 and 1436 cm^{-1} due to the presence of N–H stretching, C–H stretching, C═O stretching, N–H bending and C═C stretching vibration. The CH_2 bending, C–O stretching, and C–O–C asymmetric stretching of the molecule was assigned by the peaks 720, 1078 and 1274 cm^{-1} [18-19]. The peak at 549 cm^{-1} could be attributed to Y–O stretching mode. In the case of doped materials, the spectral peaks were slightly shifted due to

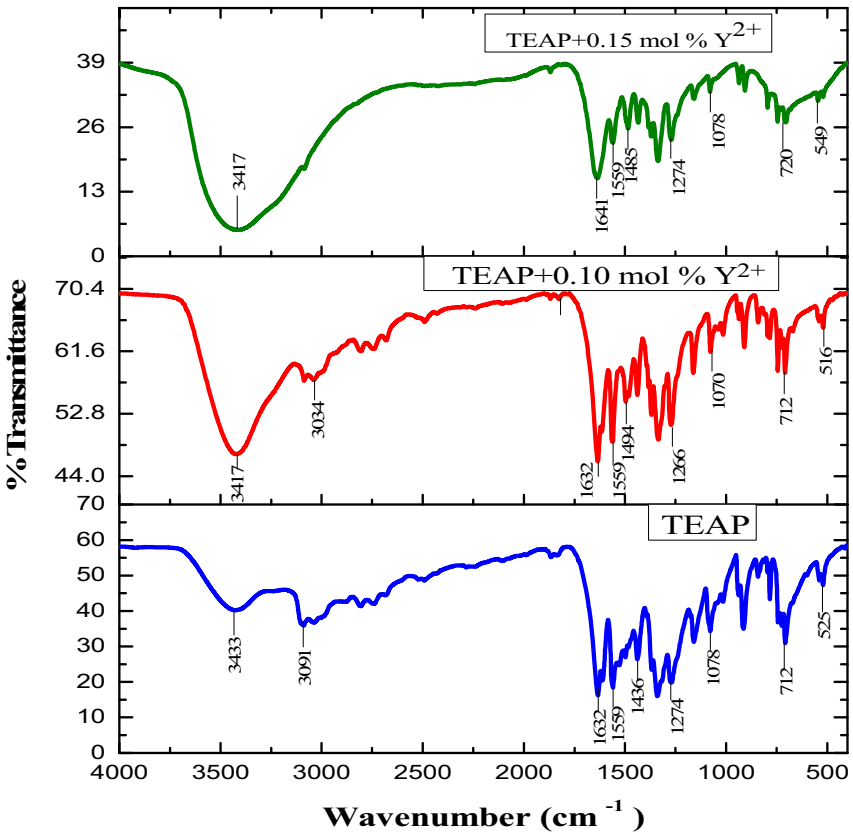

Fig. 3. FT-IR spectra of TEAP, 0.10 mol % Y^{2+} +TEAP and 0.15 mol % Y^{2+} +TEAP.

Table 2
Vibrational frequency and assignment of TEAP and doped TEAP.

Assignment	Vibration frequencies (cm^{-1})		
	0.15 mol % Y^{2+}+TEAP	0.10 mol % Y^{2+}+TEAP	TEAP
N–H Stretching	3417	3417	3433
=C–H Stretching	-	3034	3091
C=O Stretching	1641	1632	1632
N–H bending	1559	1559	1559
C=C Stretching	1485	1494	1436
=C–O–C Asymmetric Stretching	1274	1266	1274
C–O Stretching	1078	1070	1078
CH_2 bending	720	712	712
Y–O Stretching	549	516	525

the incorporation of Y^{2+} ions in pure TEAP. The vibrational frequencies and Assignments of the pure and doped materials have been given in the Table 2.

3.3. UV – visible studies

UV –Visible studies of Tri Ethyl Ammonium Picrate (TEAP), 0.10 mol % and 0.15 mol % of Y^{2+} ions doped TEAP was carried out using Thermo fisher Evolution 220 UV –Visible Spectrophotometer in the range of 190 nm–1100 nm at Alagappa University, Karaikudi as shown in Figs. 4 and 5. From the absorption spectra cut off wavelength of the materials was observed as 309.16 nm for TEAP, 307.49 nm for 0.10 mol % of Y^{2+} ions doped TEAP and 306.30 nm for 0.15 mol % of Y^{2+} ions doped TEAP respectively. The transmittance of TEAP, 0.10 mol % Y^{2+} ions and 0.15 mol % Y^{2+} ions doped TEAP crystals are 74.70 %, 83.47 % and 87.52 % in entire visible and near IR regions. This results show that the transmittance of the 0.15 mol % of Y^{2+} ions doped materials have greater value than that of TEAP and 0.10 mol % Y^{2+} ions doped materials. This increase of transmittance of the material is due to the higher concentrations of Y^{2+} ions in TEAP. By using the absorption data, the graph was plotted between hν and $(\alpha h\nu)^2$ to find the forbidden energy gap of the grown materials and as shown in Fig. 6. The obtained forbidden energy band gap of the grown materials from Tauc's plot graphs are 3.76 eV, 3.82 eV and 3.87 eV for TEAP, 0.10 mol % and 0.15 mol % of Y^{2+} ions doped TEAP crystals. UV –Visible studies results reveal that the 0.15 mol % of Y^{2+} ions doped material is a well suitable candidate for optoelectronic device applications [20, 21].

3.4. Photoluminescence studies

The Photoluminescence studies of the grown materials were carried out by using Varian Cary Eclipsc Photoluminescence spectrometer (Oxford low temperature LN277K setup) in the wavelength range between 350 nm and 600 nm. PL spectra of Tri Ethyl Ammonium Picrate (TEAP), 0.10 mol % of Y^{2+} ions doped TEAP and 0.15 mol of % Y^{2+} ions doped TEAP crystals is shown in Fig. 7. The Photoluminescence spectra exhibited a broad band from 400 nm to 475 nm with lower intensities due to the benzene ring in TEAP crystals. The excitation wavelength of the grown materials is 350 nm and the sharp emission peaks was observed at 488 nm with few additional peaks were found at 507 nm (2.45 eV), 521 nm (2.38 eV) and 552nm (2.25 eV). The sharp peak at 488 nm shows that the materials have blue emission on excitation wavelength at 350 nm. Additional peaks were observed at 507 nm, 521 nm and 552 nm are also shows that the materials have blue and green emission. Both Intensities and Wavelength of all the doped material was shifted due to the addition of Yttrium in TEAP. From the PL spectra, the sharp emission peak suggests that the grown materials are well suitable candidate to use in Photonic applications.

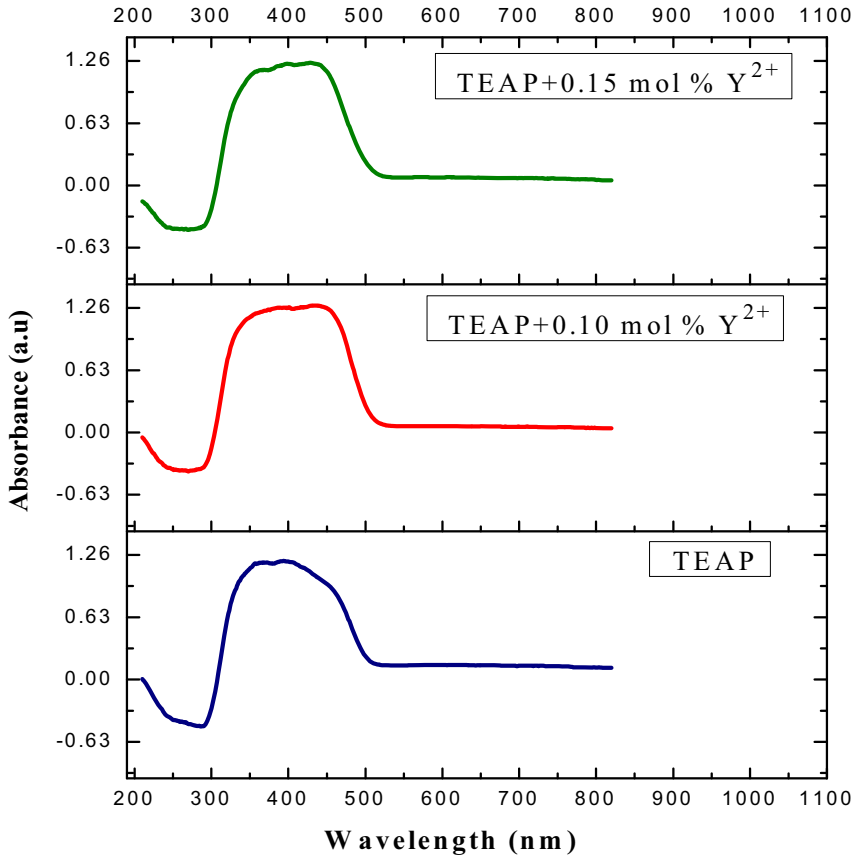

Fig. 4. UV –Vis Absorbance spectra of TEAP, 0.10 mol % Y^{2+} +TEAP and 0.15 mol % Y^{2+} +TEAP.

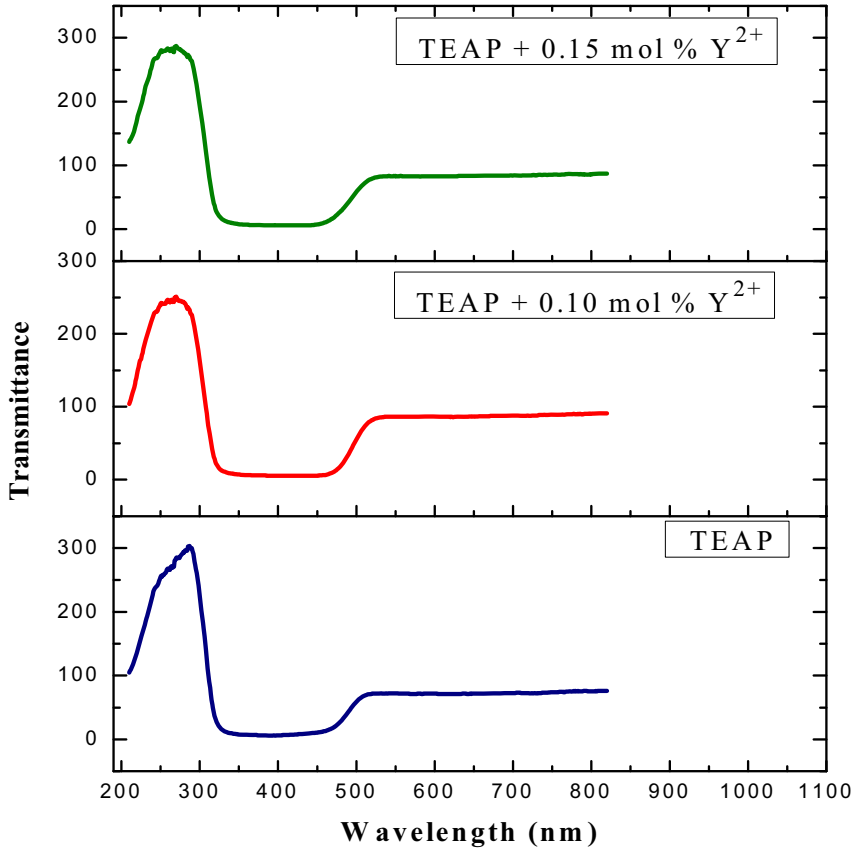

Fig. 5. UV –Vis Transmittance spectra of TEAP, 0.10 mol % Y^{2+} +TEAP and 0.15 mol % Y^{2+} + TEAP.

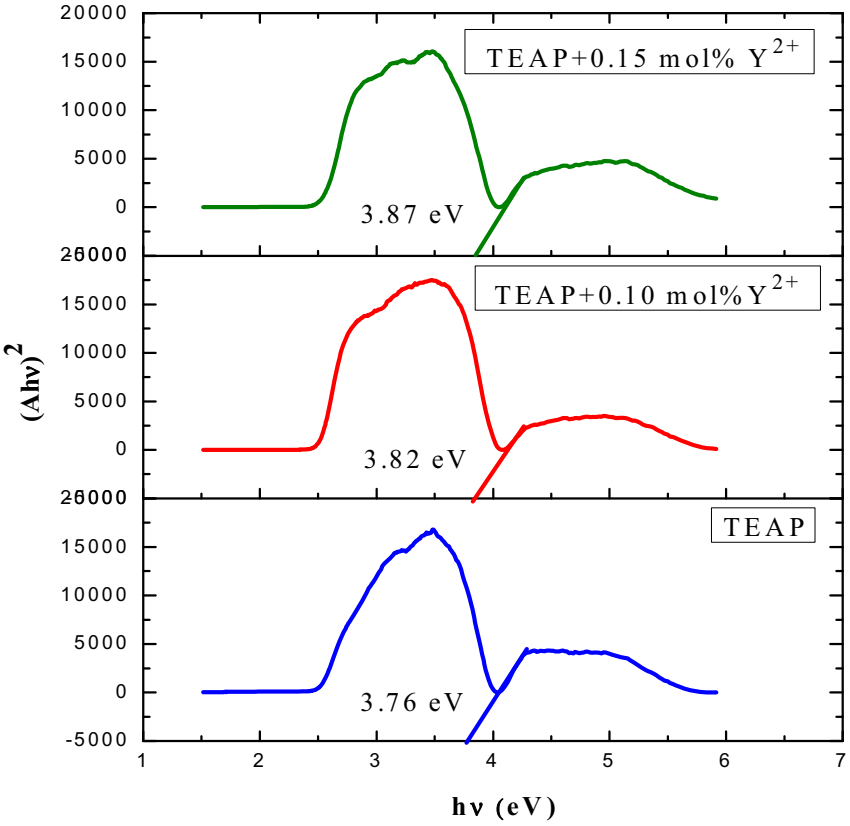

Fig. 6. hν vs $(\alpha h\nu)^2$.

3.5. EDAX analysis

Energy dispersive X-ray analysis (EDAX) is an important tool to obtain the chemical composition of the grown single crystals. Tri Ethyl Ammonium Picrate (TEAP), 0.10 mol % of Y^{2+} ions doped TEAP, 0.15 mol % of Y^{2+} ion doped TEAP single crystals was subjected to Energy dispersive X-ray analysis by using EDS BRUKER NANO GMBH D-12489 (Germany) with accelerating voltage 0–30 kV. As per the Molecular formula of TEAP ($C_{12}H_{18}N_4O_7$) and dopants (Y_2O_3), Carbon, Nitrogen, Oxygen and Yttrium elements were presented in grown materials. The EDAX spectrum of pure TEAP, 0.10 mol % and 0.15 mol % of Y^{2+} doped TEAP are exhibited in Figs. 8, 9, and 10. The atomic Wt % and Wt % of the elements of the materials are tabulated in Table 3.

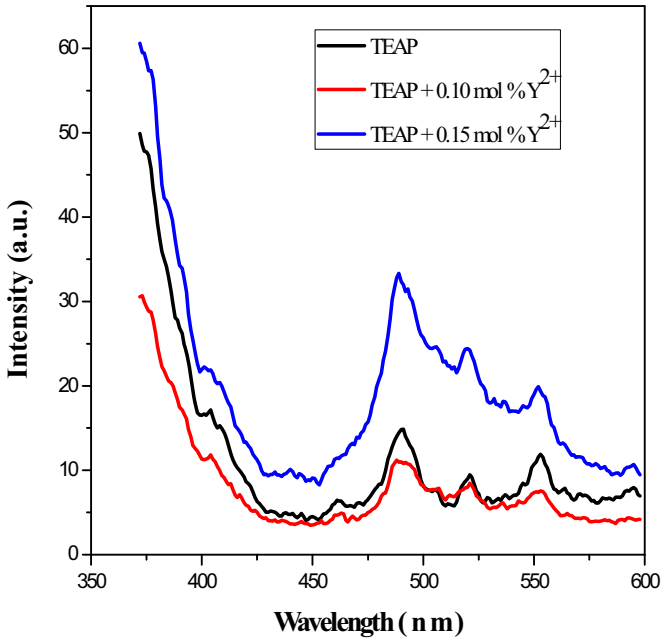

Fig. 7. Photoluminescence spectra of TEAP, 0.10 mol % Y^{2+} +TEAP and 0.15 mol % Y^{2+} +TEAP.

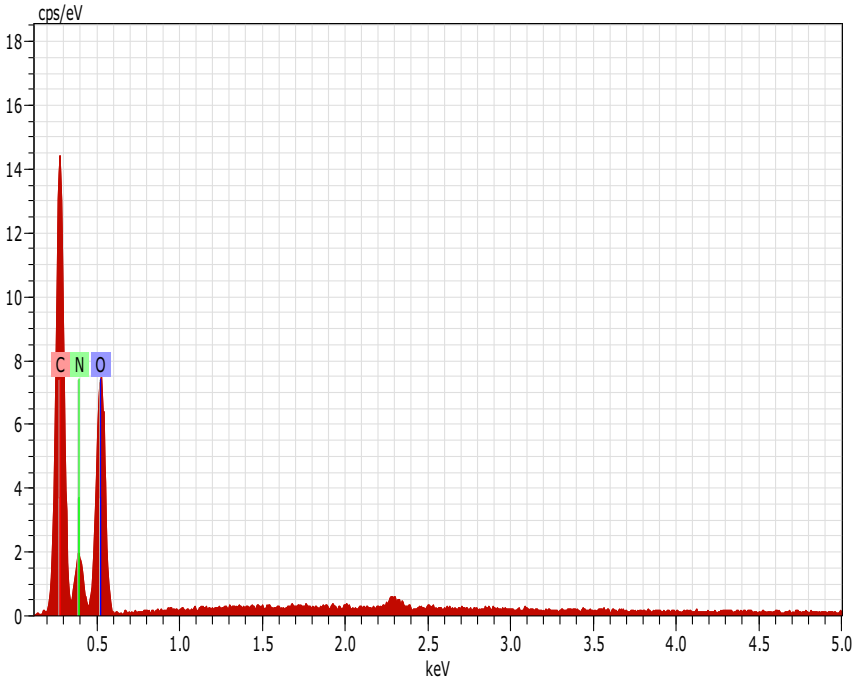

Fig. 8. EDAX spectrum of TEAP.

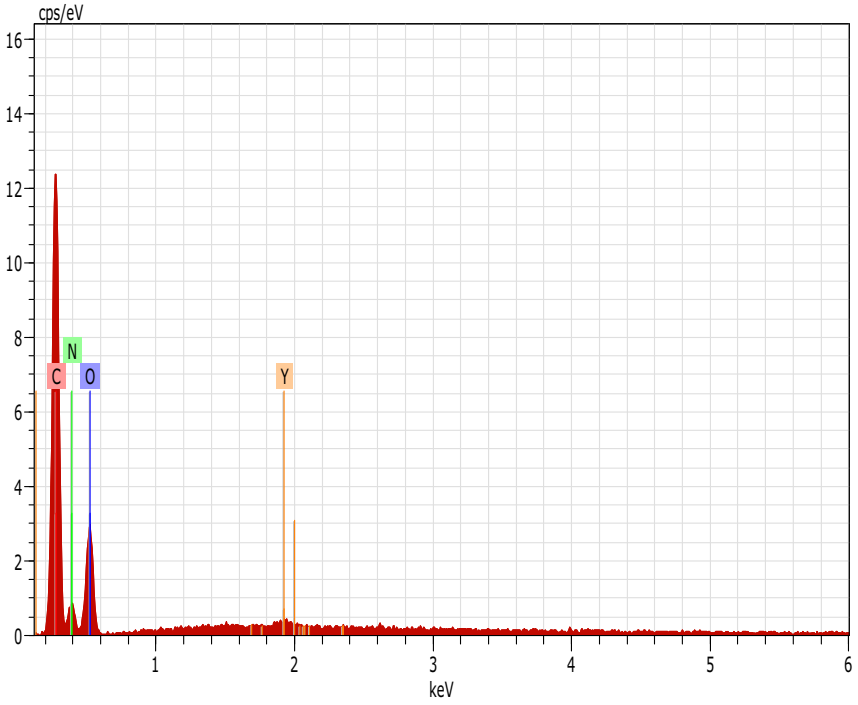

Fig. 9. EDAX spectrum of 0.10 mol% Y^{2+} +TEAP.

4. Conclusion

The single crystals of TEAP and Y^{2+} ions doped TEAP crystals were grown by slow evaporation method at room temperature. The calculated lattice parameters are a = 6.985 Å, b = 22.03 Å, c = 20.810 Å and $\alpha = \beta = \gamma = 90^{\circ}$ which confirms that the grown materials belong to crystal system of Orthorhombic. The FTIR spectral peak at 549 cm^{-1} could be attributed to Y–O stretching mode. EDAX spectra revealed the presence of elements Carbon, Nitrogen, Oxygen and Yttrium in the grown materials. The PL emission peak was observed at 488 nm. Based on the analysis report, 0.15 mol % of Y^{2+} ions doped TEAP single crystal is well suitable candidate to use in optoelectronic device applications.

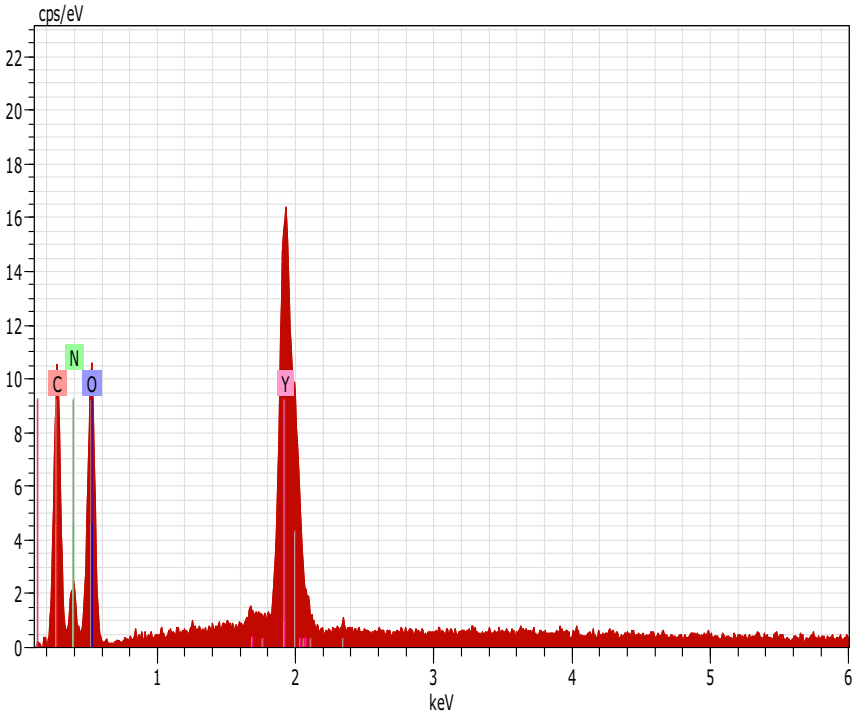

Fig. 10. EDAX spectrum of 0.15 mol % Y^{2+} +TEAP.

Table 3
Percentage of elements in TEAP and doped TEAP.

S. No.	Elements	TEAP		0.10 mol % of Y^{2+} TEAP		0.15 mol % of Y^{2+} TEAP	
		At wt%	Wt %	At wt%	Wt %	At wt%	Wt %
1	C	43.90	38.02	56.71	50.69	42.17	32.56
2	N	36.94	42.63	25.85	30.78	37.42	38.50
3	O	19.16	19.35	17.39	18.13	18.22	16.40
4	Y			0.06	0.40	2.19	12.54

Declarations

Author contribution statement

Shanmugam Velayutham: Conceived and designed the experiments; Performed the experiments; Analyzed and interpreted the data; Contributed reagents, materials, analysis tools or data.

Selvapandiyan Marimuthu: Conceived and designed the experiments; Analyzed and interpreted the data; Contributed reagents, materials, analysis tools or data; Wrote the paper.

Funding statement

This research did not receive any specific grant from funding agencies in the public, commercial, or not-for-profit sectors.

Competing interest statement

The authors declare no conflict of interest.

Additional information

No additional information is available for this paper.

Acknowledgements

The authors wish to thank Professor and Head, Department of Physics, Alagappa University, Karaikudi for Powder XRD, UV, and PL characterization facilities. The authors thank to Professor and Head, Department of Chemistry, The Gandhigram Rural Institute – Deemed University, Gandhigram – 624 302, Tamil Nadu for EDAX analysis. .

References

[1] P. Karthiga Devi, K. Venkatachalam, Structural, optical, mechanical and density functional theory studies of 1H-pyrazol-2-ium hydrogen oxalate crystal, Mater. Chem. Phys. 183 (2016) 210–219.
[2] T. Pal, T. Kar, G. Bocelli, L. Rigi, Synthesis, growth, and characterization of l-Arginine acetate crystal: a potential NLO material, Cryst. Growth Des. 3 (2003) 13–16.
[3] P. N Prasad, D.J. Willams, Introduction to Nonlinear Optical Effects on Molecules and Polymers, Wiley, New York, 1991.
[4] D.S. Chemla, J. Zyss, Nonlinear optical properties of organic molecules and crystals, 1 and 2, Academic, Orlando, 1987.
[5] W. Zhang, R.G. Xiong, Ferroelectric metal–organic frameworks, Chem. Rev. 112 (2012) 1163–1195.
[6] M. Wutting, N. Yamada, Phase-change materials for rewriteable data storage, Nat. Mater. 6 (2007) 824–832.
[7] Z.H. Sun, T.I. Chen, J.H. Luo, M.H. Hong, Bis(imidazolium) L-tartrate: a hydrogen-bonded displacive-type molecular ferroelectric material, Angew. Chem. Int. Ed. 51 (2012) 3871–3876.
[8] H.M. Zheng, J.B. Rivest, T.A. Miller, et al., Observation of transient structural - transformation dynamics in a Cu_2S nanorod, Science 333 (2011) 206–209.
[9] M. Salinga, M. Wutting, Phase-change memories on a diet, Science 332 (2011) 543–544.
[10] M.W. Gaultois, P.T. Barton, C.S. Birkel, et al., Structural disorder, magnetism, and electrical and thermoelectric properties of pyrochlore $Nd_2Ru_2O_7$, J. Phys. Condens. Matter 25 (2013) 186004.
[11] Y. In, H. Nagata, M. Doi, T. Ishida, A. Wakahara, Imidazole-4-acetic acid-picric acid (1/1) complex, Acta Crystallogr. C53 (1997) 367–369.
[12] H. Takayanagi, T. Kai, S. Yamaguchi, K. Takeda, M. Goto, Studies on picrate. VIII. Crystal and molecular structures of aromatic amine picrates : aniline, N-Methylaniline, N, N-Dimethylaniline and o-, m- and p-Phenylenediamine picrates, Chem. Pharm. Bull. 44 (1996) 2199–2204.
[13] Muhammad Adnan Asghar, Jing Zhang, Shiguo Han, Zhihua Sun, Chengmin Ji, Aurang Zeb, Junhua Luo, Triethylammonium picrate: an above-room-temperature phase transition material to switch quadratic nonlinear optical properties, Cinese Chem. Lett. 29 (2018) 285–288.

[14] J. Fraanje, K. Saminathan, C. Muthamizhchelvan, R. Peschar, K. Sivakumar, 3-Methyl anilinium picrate, Acta Crystallogr. 61 (2005) 1153–1155.
[15] G.A. Babu, A. Chandramohan, P. Ramasamy, G. Bhagavan-narayana, B. Varghese, Synthesis, structure, growth and physical properties of a novel organic NLO crystal: 1,3- Dimethylurea dimethylammonium picrate, Mater. Res. Bull. 46 (2011) 464–468.
[16] J.C. Brice, Crystal Growth Processes, John Wiley and Sons, New York, 1986.
[17] Charles Kittle, Introduction to Solid State Physics, seventh ed., Wiley India, New Delhi, 2008.
[18] Robert M. Silverstein, Francis X. Webster, David J. Kiemle, Spectrometric Identification of Organic Compounds, seventh ed., John Wiley & Sons, New York, 2005.
[19] C.N. Bandwell, Fundamentals of Molecular Spectroscopy, third ed., McGRAW-HILL Book Company, New Delhi, 1983.
[20] S. Horiuchi, Y. Tokura, Organic ferroelectrics, Nat. Mater. 7 (2008) 357–366.
[21] S.H. Baek, C.M. Folkman, J.W. Park, et al., The nature of polarization fatigue in $BiFeO_3$, Adv. Mater. 23 (2011) 1621–1625.